Published in final edited form as:
Nat Neurosci. 2008 May ; 11(5): 565–571. doi:10.1038/nn.2110.

Quantal noise from human red cone pigment

Yingbin Fu[1,3,4,5], **Vladimir Kefalov**[1,3,4,5], **Dong-Gen Luo**[1,3,5], **Tian Xue**[1,3,5], and **King-Wai Yau**[1,2,3]

[1]Solomon H. Snyder Department of Neuroscience, Room 907 Preclinical Teaching Building, 725 North Wolfe Street, Johns Hopkins University School of Medicine, Baltimore, Maryland 21205, USA

[2]Department of Ophthalmology, Room 907 Preclinical Teaching Building, 725 North Wolfe Street, Johns Hopkins University School of Medicine, Baltimore, Maryland 21205, USA

[3]Center for Sensory Biology, Room 907 Preclinical Teaching Building, 725 North Wolfe Street, Johns Hopkins University School of Medicine, Baltimore, Maryland 21205, USA

Abstract

The rod pigment, rhodopsin, shows spontaneous isomerization activity. This quantal noise produces a dark light of ~0.01 photons s^{-1} rod^{-1} in human, setting the threshold for rod vision. The spontaneous isomerization activity of human cone pigments has long remained a mystery because the effect of a single isomerized pigment molecule in cones, unlike that in rods, is small and beyond measurement. We have now overcome this problem by expressing human red cone pigment transgenically in mouse rods in order to exploit their large single-photon response, especially after genetic removal of a key negative-feedback regulation. Extrapolating the measured quantal noise of transgenic cone pigment to native human red cones, we obtained a dark rate of ~10 false events s^{-1} $cone^{-1}$, almost 10^3-fold lower than the overall dark transduction noise previously reported in primate cones. Our measurements provide a rationale for why mammalian red, green and blue cones have comparable sensitivities, unlike their amphibian counterparts.

The ability of our visual system to report light at threshold is confounded by intrinsic noise ('dark light') in the rod and cone photoreceptors[1–4]. There are at least two types of transduction noise in photoreceptors: 'quantal noise' due to spontaneous isomerization of the visual pigment[5,6], which in every way resembles real light, and 'continuous noise' originating from downstream phototransduction steps[5,7–9]. Previous recordings from single primate rods[6,10] have nicely demonstrated that the very low quantal noise from rhodopsin, corresponding to ~0.01 false event s^{-1} rod^{-1} in darkness, indeed sets the human psychophysical scotopic threshold, which likewise is low[1,3]. On the other hand, the situation with cones has so far eluded answer because individual quantal events in native cones are below resolution[11,12]. Recent work with transgenic *Xenopus laevis*[13] has provided an estimate for the thermal stability of cone pigment, but, because *Xenopus* uses A_2 pigments whereas human (and essentially all land-based animals) uses A_1 pigments, the dark quantal noise in native human cones remains

Correspondence should be addressed to K.-W.Y. (kwyau@mail.jhmi.edu).
[4]Present addresses: Department of Ophthalmology & Visual Sciences, 65 Medical Drive, University of Utah School of Medicine, Salt Lake City, Utah 84132, USA (Y.F.) and Department of Ophthalmology & Visual Sciences, 660 S. Euclid, Washington University School of Medicine, St. Louis, Missouri 63110, USA (V.K.).
[5]These authors contributed equally to this work.

Note: Supplementary information is available on the Nature Neuroscience website.

a mystery. We have now successfully addressed this question in experiments with transgenic mice, enabling us to deduce the quantal noise in human red cones.

RESULTS

Transgenic expression of red cone opsin in mouse rods

We generated a mouse line (*OPN1LW*$^{+}$*Rho*$^{+/+}$) expressing human red cone opsin (OPN1LW) under the control of the mouse rhodopsin promoter (Fig. 1a). At 1 month of age, this mouse's retina had normal-looking outer-segment and outer-nuclear layers (Fig. 1b). Immunostaining for red cone opsin labeled the rod outer segments abundantly, coinciding with that for rhodopsin (Fig. 1b). Crossing the *OPN1LW*$^{+}$*Rho*$^{+/+}$ line with the *Rho*$^{-/-}$ (rhodopsin-knockout) line[14] gave *OPN1LW*$^{+}$*Rho*$^{+/-}$, then *OPN1LW*$^{+}$*Rho*$^{-/-}$, mice. The *OPN1LW*$^{+}$*Rho*$^{+/-}$ retina was similar to the *Rho*$^{+/-}$ retina, with mild degeneration (data not shown). *Rho*$^{-/-}$ retina lacks the outer segment layer[14], but *OPN1LW*$^{+}$ *Rho*$^{-/-}$ retina even at 2 months of age retains this layer, although it is thin from substantial rod degeneration (Fig. 1c). The colocalization of immunolabelings for red cone opsin and the rod cyclic nucleotide–gated channel subunit A (CNGA1) confirmed the correct targeting of the transgenic pigment to the surviving rods' outer segments in the *OPN1LW*$^{+}$*Rho*$^{-/-}$ retina (Fig. 1c).

OPN1LW^{+}*Rho*$^{-/-}$ rods gave light responses very similar to wild type (*Rho*$^{+/+}$) (Fig. 2a) but, as expected, showed an action spectrum consistent with the absorption spectrum of human red cone pigment, with λ_{max} at 557 nm (Fig. 2b; see legend). Variance analysis of dim-flash responses indicated similar amplitudes of the single-photon responses in *OPN1LW*$^{+}$*Rho*$^{-/-}$ rods and *Rho*$^{+/+}$ rods (0.35 pA versus 0.40 pA; Table 1). We also compared the signaling properties between endogenous rhodopsin and transgenic cone pigment in a given *OPN1LW*$^{+}$*Rho*$^{+/+}$ or *OPN1LW*$^{+}$*Rho*$^{+/-}$ rod by taking advantage of the spectral separation between the two pigments. It will be shown below that the transgenic cone pigment was expressed at a very low level, so <600-nm light would stimulate rhodopsin predominantly whereas 690-nm light would stimulate the cone pigment with substantial probability (0.37 for *OPN1LW*$^{+}$*Rho*$^{+/+}$ and 0.54 for *OPN1LW*$^{+}$*Rho*$^{+/-}$ rods). Nonetheless, neither the single-photon response amplitude (estimated from variance analysis) nor the kinetics (time to peak and integration time) of the dim-flash response of *OPN1LW*$^{+}$ *Rho*$^{+/+}$ and *OPN1LW*$^{+}$*Rho*$^{+/-}$ rods varied with the stimulating wavelength (Supplementary Fig. 1 online), being similar to that found for the *Rho*$^{+/+}$ and *Rho*$^{+/-}$ phenotypes, respectively. Thus, rhodopsin and red cone pigment signaled identically in a given cell, consistent with our previous finding[13] on A_2 pigments in transgenic *Xenopus*.

Expression level of human red cone pigment

Given that rod and cone pigments triggered identical responses in a rod, the percentage red cone pigment in *OPN1LW*$^{+}$*Rho*$^{+/+}$ rods could be estimated from the red shift in the action spectrum. A best fit to the averaged spectrum with a linear combination of the absorptionspectrum templates for the two pigments yielded 0.25% red cone pigment in *OPN1LW*$^{+}$*Rho*$^{+/+}$ rods (Fig. 3a, left; 11 cells). *OPN1LW*$^{+}$ *Rho*$^{+/-}$ rods showed a larger red shift (Fig. 3a, right, 14 cells), yielding 0.5% red cone pigment, as expected from the lower (50% of wild-type value) rhodopsin level in *OPN1LW*$^{+}$ *Rho*$^{+/-}$ rods[14]. Thus, the expression of red cone pigment was low and did not increase even when the endogenous rhodopsin level decreased, explaining the eventual degeneration of *OPN1LW*$^{+}$ *Rho*$^{-/-}$ rod outer segments, which had no rhodopsin.

Because of the importance of the percentage estimate in subsequent calculations, we checked the cone-pigment expression level with a second method, by using the *Sag*$^{-/-}$ genetic background[15], which removes the inactivation of photoisomerized pigment by arrestin and

thus reveals the intrinsic decay of the active meta-II state of the pigment. The dim-flash responses of *Rho*$^{+/+}$*Sag*$^{-/-}$ and *OPN1LW*$^{+}$*Rho*$^{-/-}$*Sag*$^{-/-}$ rods (Fig. 3b, left and middle) showed a comparably rapid initial decline, reflecting similar time courses of phosphorylation of the meta-II states of rhodopsin and red cone pigment in the rod environment. This initial decline was followed by a slower decline that reflected the decay of each pigment's meta-II state, measured to be, in time constant, 46.0 ± 8.3 s (9 cells) for mouse rhodopsin and 0.62 ± 0.05 s (18 cells) for human red cone pigment, a ~70-fold difference that was broadly similar to previous *in vitro* measurements[16]. Regarding the *OPN1LW*$^{+}$*Rho*$^{+/-}$*Sag*$^{-/-}$ rod (Fig. 3b, right), the slow decay of its dim-flash response at 500 nm was essentially identical to the *Rho*$^{+/+}$*Sag*$^{-/-}$ phenotype, as expected from the literally exclusive stimulation of rhodopsin (see above); at 690 nm, however, a significant fraction of the response was due to the cone pigment, resulting in a composite slow response decay contributed by both pigments. From the ratio of the initial amplitudes of the two components in the composite decay (reflecting the photoactivated rhodopsin:red cone pigment ratio) and the absorption-spectrum templates for the two pigments (Fig. 2b), the percentage red cone pigment in the cell could be calculated (Fig. 3b; see Methods). Collective results gave 0.65 ± 0.15% for *OPN1LW*$^{+}$*Rho*$^{+/-}$*Sag*$^{-/-}$ rods (11 cells). Similar experiments on *OPN1LW*$^{+}$*Rho*$^{+/+}$*Sag*$^{-/-}$ rods (11 cells) gave 0.26 ± 0.05% red cone pigment (not shown). These values agreed well with those derived from the red shifts in the spectral sensitivities of *OPN1LW*$^{+}$*Rho*$^{+/-}$ and *OPN1LW*$^{+}$*Rho*$^{+/+}$ rods.

Rate of thermal isomerization of red cone pigment

We next proceeded to measure the isomerization rate of red cone pigment in darkness. The single-photon response in mouse rods is not large enough for unambiguous resolution from the continuous noise[17]. Accordingly, we crossed *OPN1LW*$^{+}$*Rho*$^{+/+}$ mice with *Guca1a*$^{-/-}$ *Guca1b*$^{-/-}$(*Gcaps*$^{-/-}$) mice[18]. In the *Gcaps*$^{-/-}$ background, a major negative feedback on phototransduction (through the GCAPs, or guanylate cyclase–activating proteins) is removed, resulting in a ~ 5-fold increase in the single-photon response amplitude[17]. The *Gcaps*$^{-/-}$ background did not affect retinal morphology, nor the red cone pigment's localization (Fig. 4) and expression level, the latter being estimated to be 0.26% (16 cells) in *OPN1LW*$^{+}$*Rho*$^{+/+}$*Gcaps*$^{-/-}$ rods on the basis of the average red shift in the action spectrum (Fig. 4).

We used three methods to measure the rate of spontaneous isomerization in these rods. The first was to identify and count the quantal events (marked by asterisks in sample records in Fig. 5a) in long recordings in darkness, based on a criterion amplitude at > 30% of the single-photon response amplitude (this parameter being derived by variance analysis of dim-flash responses from the same cell) and a criterion integration time within the 50–200% range of the average dim-flash response. The substantial fluctuations in event amplitude presumably arose from the removal of the GCAPs negative feedback. We arrived at a rate of 0.013 ± 0.002 isomerizations (R*) s^{-1} (20 cells) for *Rho*$^{+/+}$ *Gcaps*$^{-/-}$ rods (control) and 0.033 ± 0.006 R* s^{-1} (26 cells) for *OPN1LW*$^{+}$*Rho*$^{+/+}$*Gcaps*$^{-/-}$ rods. The rate was 0.018 R* s^{-1} for the top cell and 0.035 R* s^{-1} for the bottom cell in Figure 5a. The control rate was similar to a previous estimate (0.012 R* s^{-1}) for thermal isomerization of rhodopsin in mouse rods[17]. The difference between the two average rates gave 0.020 R* s^{-1} attributed to red cone pigment.

The second method was based on power density spectra computed from overall dark recordings and from selected segments of recordings showing no obvious quantal events[5] (see Methods). By fitting the square of the Fourier transform of the single-photon response function to the difference spectrum (that is, spectrum with quantal events minus spectrum without quantal events) (Fig. 5b), we obtained 0.020 ± 0.002 R* s^{-1} (two cells) for *Rho*$^{+/+}$ *Gcaps*$^{-/-}$ rods and 0.062 ± 0.023 R* sec^{-1} (five cells) for *OPN1LW*$^{+}$*Rho*$^{+/+}$*Gcaps*$^{-/-}$ rods, giving 0.042 R* s^{-1}

for the red cone pigment. The rate was 0.018 R* s^{-1} for the top cell and 0.037 R* s^{-1} for the bottom cell in Figure 5b.

The third method was based on probability density histograms[5]. We computed a probability density histogram from overall dark recordings (Fig. 5c, red profile). The profile was almost symmetrical about 0 pA, except for some excess probability predominantly in the 0.5–5 pA range that reflected the presence of quantal events in darkness. Indeed, segments of recording with no obvious quantal events gave a symmetrical probability density histogram, as expected (Fig. 5c, blue profile; see Methods). From the excess (that is, asymmetrical) probability density, we calculated the dark event rate as 0.014 ± 0.003 R* s^{-1} (10 cells) for *Rho*$^{+/+}$ *Gcaps*$^{-/-}$ rods and 0.036 ± 0.006 R* s^{-1} (13 cells) for *OPN1LW*$^{+}$*Rho*$^{+/+}$*Gcaps*$^{-/-}$ rods, giving 0.022 R* s^{-1} for the red cone pigment. The rate was 0.022 R* s^{-1} for the top cell and 0.042 R* s^{-1} for the bottom cell in Figure 5c. This method is the most objective because, other than the assumption of the background noise being symmetrical, no selection of recordings is necessary.

We adopted the estimate from probability density histograms for later calculations, yielding a normalized 0.088 R* s^{-1} per 1% red cone pigment in the rod (obtained by dividing the above value by 0.25%, the average percentage transgenic red cone pigment in *OPN1LW*$^{+}$*Rho*$^{+/+}$ and *OPN1LW*$^{+}$*Rho*$^{+/+}$*Gcaps*$^{-/-}$ rods). Transgene expression was not exactly constant across the retina[19]. For three *OPN1LW*$^{+}$*Rho*$^{+/+}$ *Gcaps*$^{-/-}$ rods, we were able to measure the cone-pigment expression level as well as the extra isomerization rate in darkness. They were roughly linearly related, with a slope of 0.072 R* s^{-1} per 1% red cone pigment (Fig. 4c, probability-density method). Finally, we compared the profiles of the averaged excess probability density histograms for *Rho*$^{+/+}$ *Gcaps*$^{-/-}$ rods and *OPN1LW*$^{+}$*Rho*$^{+/+}$*Gcaps*$^{-/-}$ rods (Fig. 5d). The two profiles were essentially identical, further supporting the notion that the rhodopsintriggered events and the red cone pigment-triggered events had similar amplitudes and kinetics.

Adaptation of mouse rods to background light

We examined the adaptation of *Rho*$^{+/+}$ (that is, wild type) mouse rods to background light, to evaluate the desensitizing effect of spontaneous isomerization of transgenic red cone pigment in a rod. The experiment consisted of measuring the dim-flash sensitivity of a rod (dim-flash response amplitude divided by flash intensity) at different levels of background light. The collected data, plotted as normalized flash sensitivity against the number of isomerizations due to background light intensity (Fig. 6), showed that it required ~35 R* s^{-1} to reduce the dim-flash sensitivity of mouse rods by half (calculated by assuming an effective outer-segment collecting area of 0.35 μm^2 under our experimental conditions[20,21]). This value is very similar to the ~ 30–50 R* s^{-1} previously found for rat and other mammals, including primate[21,22]. It is therefore not surprising that an average spontaneous activity of 0.022 R* s^{-1} due to transgenic red cone pigment in *OPN1LW*$^{+}$*Rho*$^{+/+}$ rods did not decrease the dim-flash sensitivity compared to that of *Rho*$^{+/+}$ rods (Table 1 and Supplementary Fig. 1).

DISCUSSION

We expressed transgenically human red cone pigment in mouse rods, which allowed us to exploit the high amplification in rod phototransduction for detecting the effect of a single isomerized cone pigment molecule. Mouse, like human, uses vitamin A1 as the chromophore for its visual pigments. In this way, we were able to determine the rate of thermal isomerization of A_1 red cone pigment. This determination of isomerization rate required the measurement of the amount of transgenic pigment expression and its associated quantal noise in darkness. The expression was measured on the basis of either one of two differences in property between red cone pigment and rhodopsin, the first being red cone pigment's higher absorbance at long wavelengths and the second being the much faster decay of the cone pigment's meta-II state. Both methods gave ~0.25% of the pigment in an *OPN1LW*$^{+}$*Rho*$^{+/+}$ rod being red cone pigment.

To measure the associated quantal noise, we bred the transgenic *OPN1LW*$^{+}$*Rho*$^{+/+}$ line to a *Gcaps*$^{-/-}$ background in order to eliminate a key Ca^{2+} feedback on phototransduction through the GCAP proteins and thus further boost the single-photon response to an amplitude large enough for detection[17,18]. Three independent methods (based on counting, power spectrum, and probability density, respectively) yielded similar thermal isomerization rates attributed to the red cone pigment in a transgenic rod, being ~ 0.088 R* s^{-1} per 1% of total pigment in a mouse rod as cone pigment. A mouse rod has ~6.5×10^7 pigment molecules (see Methods). Thus, the molecular rate constant of thermal isomerization for A_1 human red cone pigment is ~ (0.088 R* s^{-1}) / (6.5×10^7 R × 0.01) = 1.35×10^{-7} s^{-1} (37 °C). The pigment content of a primate red cone is about the same as that of a mouse rod (Methods); hence, the spontaneous isomerization rate in a primate red cone at 37 °C should be ~ 8.8 R* s^{-1}. Previously[11,12], the variance of the overall dark noise (before optimal filtering) in a primate red cone outer segment had been found to be extremely high, equivalent to 6,400 R* s^{-1}, or almost 1,000-fold higher than the dark quantal noise we measured here. Thus, the overwhelming amount of dark noise in the primate red cone originates not from spontaneous isomerization of the pigment, but most probably from constitutive activity in the downstream phototransduction steps, such as the phosphodiesterase[9]. The psychophysical dark light at the fovea was estimated[2] to be 10^3–10^4 times that of rods, or 10–100 R* s^{-1} $cone^{-1}$ (given that it is ~0.01 R* s^{-1} for a rod; see Introduction). Other authors[3] have likewise arrived at a dark-light value of ~ 100 R* s^{-1} per foveal cone. Thus, the quantal noise we measured is much closer than the overall transduction noise to this psychophysical photopic threshold. Although we studied only human red cone pigment and therefore the data apply only to red cones, we expect the dark quantal rates to be no higher in green and blue cones[23–25]. Thus, notably, the cone quantal noise appears to be much closer than the overall noise to the psychophysical photopic dark light. One possibility is that the visual pathway manages to suppress the overwhelming non-quantal noise, a surprising feat, if true, considering the small size of the single-photon response in cones as well as the rather similar frequency characteristics of the quantal and non-quantal noise (see ref [11]). Another possibility, perhaps more likely, is that the approximate match is just a coincidence, with the psychophysical dark light merely representing the residual level of combined quantal and non-quantal noise after filtering by the visual pathway.

Extrapolating the previously measured[13] molecular rate constant for thermal isomerization of A_2 human red cone pigment (6.9×10^{-7} s^{-1}) at room temperature to that at 37 °C by assuming the published temperature coefficient[26], we obtained ~5.6×10^{-6} s^{-1}, compared to ~ 1.35×10^{-7} s^{-1} derived above for its A_1 counterpart. Thus, A_1 red cone pigment is perhaps 40-fold less prone to spontaneous isomerization than the A_2 form. This is probably because the A_2 chromophore has an extra double bond in the β-ionone ring, which has been suggested to lower the energy barrier for isomerization[27]. Consequently, this introduces a red shift in absorption[28] and decreases the thermal stability of the A_2 pigment. Incidentally, a very recent paper[29] has reported that, in salamander, A_1 rhodopsin is > 30 times more stable than A_2 rhodopsin (as opposed to a previously reported ~ 10-fold[28]), rather similar to our finding here for red cone pigment. More importantly, unlike the case in lower vertebrates such as salamander, where A_2 red cone pigment is sufficiently noisy as to impose a potential adaptational influence on cones even in darkness[13,23,30], A_1 red cone pigment (and likewise green and blue cone pigments; see earlier) in primates and presumably other mammals should be quiet enough to have hardly any adaptational influence on cone sensitivity (**Supplementary Note** online; see also ref. [31]). In other words, the much lower absolute sensitivity of mammalian cones compared to mammalian rods seems to arise not from quantal noise in the pigments themselves, but from other phototransduction steps[32–34]. This may explain why primate red, green and blue cones, unlike their amphibian counterparts[35,36], all have similar sensitivities, irrespectively of their difference in visual pigments[11].

METHODS

Generation of transgenic mice

The transgene was prepared by assembling the 4.4-kb KpnI–XhoI mouse opsin promoter[19], the 95-bp third intron of human rhodopsin gene (for improving expression), and the 1.3-kb EcoRI fragment of human red cone opsin cDNA into pBluescript II KS (Fig. 1a). We microinjected the 5.8-kb fusion gene into the pronuclei of C57BL6/J × DBA/2J F_1 hybrid mouse embryos. Transgenic mice were generated by standard procedures at the transgenic mouse facility of Johns Hopkins University School of Medicine. Animal experiments were conducted according to protocols approved by the Johns Hopkins University Institutional Animal Care and Use Committee. Transgene-positive mice were identified by selective amplification of the transgene by PCR with a 5′ primer (5′-CCAGCACTATCAGCATTGT GAACC-3′) and a 3′ primer (5′-TCAAAGGGTGGAAGGCGTAACC-3′). Several transgenic lines were screened for the one with the best expression; this line was used in all experiments here. Transgene-positive mice (*OPN1LW*$^{+}$*Rho*$^{+/+}$) were bred with *Rho*$^{-/-}$ mice[14] to obtain *OPN1LW*$^{+}$*Rho*$^{+/-}$ and *OPN1LW*$^{+}$*Rho*$^{-/-}$ lines. *OPN1LW+Rho*$^{+/+}$*Sag*$^{-/-}$, *OPN1LW*$^{+}$*Rho*$^{+/-}$ *Sag*$^{-/-}$ and *OPN1LW*$^{+}$*Rho*$^{-/-}$*Sag*$^{-/-}$ mice were generated by crossing *OPN1LW*$^{+}$ R*ho*$^{+/+}$ and *OPN1LW*$^{+}$*Rho*$^{-/-}$ mice with *Sag*$^{-/-}$ mice[15]. *OPN1LW*$^{+}$*Rho*$^{+/+}$*Gcaps*$^{-/-}$ mice were generated by crossing *OPN1LW*$^{+}$*Rho*$^{+/+}$ with *Rho*$^{+/+}$*Gcaps*$^{-/-}$ mice[18]. All mice with the *Sag*$^{-/-}$ background were reared from birth in constant darkness in order to prevent light damage to the photoreceptors. All other mice were kept in a 12 h/12 h light/dark cycle.

Immunocytochemistry

Fresh eyecups were fixed overnight at 4 °C in PBS containing 4% paraformaldehyde. After further incubation overnight in PBS/30% sucrose at 4 °C, the eyecups were embedded in OCT (Tissue-Tek) and sectioned at 10–20 mm thickness. The retinal sections were processed for double immunostaining with the polyclonal antibody JH492 to red cone opsin[37] and the monoclonal antibody 1D4 to rhodopsin[38], followed by Cy3-conjugated goat antibody to rabbit IgG and Cy2-conjugated goat antibody to mouse IgG. For immunostaining of the *Rho*$^{-/-}$ and *OPN1LW*$^{+}$*Rho*$^{-/-}$ mouse eyes, we used the monoclonal antibody 1D1 to rod CNGA1 subunit[39] instead of 1D4 because rhodopsin is absent.

Electrical recordings

For *OPN1LW*$^{+}$*Rho*$^{-/-}$ and *OPN1LW*$^{+}$*Rho*$^{-/-}$*Sag*$^{-/-}$ mice, we used 1-month-old mice in order to minimize photoreceptor degeneration. For all other lines, we used 1- to 3-month-old mice. Tissue preparation and recordings were as described elsewhere[20]. Briefly, an animal dark-adapted overnight was put to death by CO_2 asphyxiation and the eyes were removed under dim red light. All subsequent manipulations were performed under infrared light. The eyes were hemisected, and the retinas removed from the pigment epithelium and chopped into small pieces with a razor blade in ice-chilled L-15 medium (0.1% BSA) pre-bubbled with 100% O_2, then transferred to the experimental chamber perfused with bicarbonate-buffered solution (in mM: 112.5 NaCl, 3.6 KCl, 2.4 $MgCl_2$, 1.2 $CaCl_2$, 10 HEPES buffer, pH 7.4, 20 $NaHCO_3$, 3 sodium succinate, 0.5 sodium glutamate, 0.02 EDTA, 10 glucose, and 0.1% BME vitamin and amino acid supplements (Sigma)). The solution was bubbled with 95% O_2/5% CO_2, and warmed to 37 °C before entering the chamber. Membrane current was recorded with a suction pipette from a rod outer segment projecting from a piece of retina. The recording electrode was filled with (in mM) 140 NaCl, 3.6 KCl, 2.4 $MgCl_2$, 1.2 $CaCl_2$, 3 HEPES, pH 7.4, 0.02 EDTA and 10 glucose. Monochromatic 10- or 20-ms flashes were used for stimulation. The signals for the experiments in Figure 2– Figure 4 and Figure 6 were low-pass filtered at 30 Hz (eight-pole Bessel) and digitized at 1 kHz. Those for the experiments in Figure 5 were low-pass filtered at 20 Hz (eight-pole Bessel) and digitized at 500 Hz or 2.5 kHz, except

for power spectral analysis, in which the signals were low-pass filtered at 20 Hz (eight-pole Butterworth) and digitized at 2.5 kHz. All indicated margins of error represent s.e.m.

In Figure 3b, right panel, the wavelengths of stimulation were alternated to avoid systematic error due to recording drift or cell deterioration. The considerably faster decay of cone pigment meta-II compared to rhodopsin meta-II resulted in a more substantial initial recovery of the response at 690 nm compared to 500 nm. Because the responses at 500 nm and 690 nm are normalized to the same height and the signaling properties of rhodopsin meta-II and red cone pigment meta-II are identical, the initial amplitude of the overall meta-II decay at 690 nm is simply the same as the initial amplitude of the rhodopsin meta-II decay at 500 nm (see main text). The initial amplitude of the rhodopsin meta-II decay in the composite decline at 690 nm can be obtained from a scaled fit by the exponential decay from the 500-nm response (τ = 54 sec). The difference then gives the initial amplitude of the cone pigment meta-II decay. The ratio of the initial amplitudes of the two decay components gives an activated rhodopsin:red cone pigment ratio of 67%/33%, which, together with the absorption-spectrum templates for rhodopsin and red cone pigment (Fig. 2a), gives 0.82% transgenic red cone pigment in this cell. In Figure 4b, because of the long recording time generally required for rods on *Gcaps*$^{-/-}$ background[18], not all indicated wavelengths were examined for every cell, except for the 500 nm and 700 nm wavelengths that were used for estimating the percentage of red cone pigment.

Single-photon response, power spectrum, and probability density histogram

The amplitude of the single-photon response was calculated as the ensemble variance:mean ratio of the transient peak amplitude of the responses to a series of 30–50 identical dim flashes. The averaged dim-flash response profile bearing the single-photon response amplitude thus represents the average single-photon response function ($f(t)$; see below).

In experiments involving power density spectrum and probability density, continuous recordings lasting minutes were made in darkness. The averaged power density spectrum was calculated from this recording by using Clampfit 9 (Axon Instruments) in 8.192-s segments with 50% overlap. Segments with no obvious quantal events (based on visual inspection) were selected and the averaged spectrum recalculated. The difference ('difference spectrum') between the two spectra represented the power spectrum for the quantal events. The power spectrum (that is, square of the Fourier transform) of the average singlephoton response function for the same cell ($f(t)$; see above) was calculated and scaled to fit the difference spectrum. The rate of spontaneous isomerization is equal to the scaling factor for the fit divided by the acquisition time (8.192 s). Finally, a stretch of recordings was also made in saturating light for each cell in order to measure the resistive noise and instrumentation noise (see below).

The probability density histograms were calculated from the same recording sweeps described above and plotted with a 0.1-pA bin width. From Campbell's theorems[5] and the definition of probability density, we have

$$\text{Mean current} = v_{\mathrm{d}} \int f(t)\mathrm{d}t = \int jp(j)\mathrm{d}j = \sum\nolimits_i [\, j(i) \times p(i)]$$

where v_{d} is the spontaneous isomerization rate and i = 1, 2, 3,… is the bin number in the probability density histogram, each with probability $p(i)$. $\int f(t)\mathrm{d}t$ is the area under the single-photon response function. The term on the right side of the equation can be calculated as the excess probability density in each amplitude bin on the positive side of the histogram (simply by folding the negative side of the histogram onto the positive side and taking the difference in probability density for a given positive-amplitude bin) multiplied by the current amplitude

for that bin, followed by summing over all positive bins. We then calculated ν_d as $\{\Sigma_i [j(i) \times p(i)]\}/\int f(t)dt$ Finally, from the difference in variance between the probability histogram for recordings with no obvious quantal events and that for recordings in bright light, we obtained the variance of the continuous noise. This variance was similar between *Rho*$^{+/+}$*Gcaps*$^{-/-}$ rods (0.28 ± 0.07 pA^2, three cells) and *OPN1LW*$^+$ *Rho*$^{+/+}$*Gcaps*$^{-/-}$ rods (0.39 ± 0.12 pA^2, four cells), further indicating that the quantal events originating from red cone pigment in *OPN1LW*$^+$*Rho*$^{+/+}$ *Gcaps*$^{-/-}$ rods were not so small as to have escaped inclusion in the visual-counting and power-spectral methods.

Calculations of pigment content in mouse rods and primate red cones

For a mouse rod outer segment of 1.4 mm in diameter and 20 mm in length[20], which gives an outer-segment volume of 30 μm^3 , the number of rhodopsin molecules (~ 3.5 mM; ref. [40]) is ~ 6.5 × 10^7. The outer-segment volume for the primate red cone is about the same[11], thus giving a similar number of cone pigment molecules per cell. These values are only approximate, with accuracy probably within a factor of two.

Supplementary Material

Refer to Web version on PubMed Central for supplementary material.

Acknowledgments

We thank J. Lai for help in generating the transgene construct, Y. Liang, L. Ding, and Y. Wang for mouse genotyping, J. Chen (University of Southern California School of Medicine) for the *Gcaps*$^{-/-}$ and *Sag*$^{-/-}$ mice and J. Lem (Tufts University School of Medicine) for the *Rho*$^{-/-}$ mice, as well as J. Nathans (Johns Hopkins University School of Medicine) and R. Molday (University of British Columbia) for their gifts of antibodies. We are indebted to P. Ala-Laurila, D. Baylor, and J. Schnapf for discussions. This work was supported by grant EY 06837 from the US National Eye Institute to K.-W.Y

References

1. Barlow HB. Increment thresholds at low intensities considered as signal/noise discriminations. J. Physiol. (Lond.) 1957;136:469–488. [PubMed: 13429514]
2. Barlow, HB. Visual Problems of Colour. Vol. Vol. II. London: Her Majesty's Stationery Office; 1958. Intrinsic noise of cones; p. 617-630.(ed. National Physical Laboratory, Teddington, England)
3. Donner K. Noise and the absolute thresholds of cone and rod vision. Vision Res 1992;32:853–866. [PubMed: 1604854]
4. Field GD, Sampath AP, Rieke F. Retinal processing near absolute threshold: from behaviour to mechanism. Annu. Rev. Physiol 2005;67:491–514. [PubMed: 15709967]
5. Baylor DA, Matthews G, Yau K-W. Two components of electrical dark noise in toad rod outer segments. J. Physiol. (Lond.) 1980;309:591–621. [PubMed: 6788941]
6. Baylor DA, Nunn BJ, Schnapf JL. The photocurrent, noise & spectral sensitivity of rods of the monkey *Macaca fascicularis*. J. Physiol. (Lond.) 1984;357:575–607. [PubMed: 6512705]
7. Rieke F, Baylor DA. Molecular origin of continuous dark noise in rod photoreceptors. Biophys. J 1996;71:2553–2572. [PubMed: 8913594]
8. Lamb TD, Simon EJ. Analysis of electrical noise in turtle cones. J. Physiol. (Lond.) 1977;272:435–468. [PubMed: 592199]
9. Holcman D, Korenbrot JI. The limit of photoreceptor sensitivity: molecular mechanisms of dark noise in retinal cones. J. Gen. Physiol 2005;125:641–660. [PubMed: 15928405]
10. Schneeweis DM, Schnapf JL. Noise and light adaptation in rods of the macaque monkey. Vis. Neurosci 2000;17:659–666. [PubMed: 11153647]
11. Schnapf JL, Nunn BJ, Meister M, Baylor DA. Visual transduction in cones of the monkey *Macaca fascicularis*. J. Physiol. (Lond.) 1990;427:681–713. [PubMed: 2100987]

12. Schneeweis DM, Schnapf JL. The photovoltage of macaque cone photoreceptors: adaptation, noise, and kinetics. J. Neurosci 1999;19:1203–1216. [PubMed: 9952398]
13. Kefalov V, Fu Y, Marsh-Armstrong N, Yau K-W. Role of visual pigment properties in rod and cone phototransduction. Nature 2003;425:526–531. [PubMed: 14523449]
14. Lem J, et al. Morphological, physiological, and biochemical changes in rhodopsin knockout mice. Proc. Natl. Acad. Sci. USA 1999;96:736–741. [PubMed: 9892703]
15. Xu J, et al. Prolonged photoresponses in transgenic mouse rods lacking arrestin. Nature 1997;389:505–509. [PubMed: 9333241]
16. Okada T, et al. Circular dichroism of metaiodopsin II and its binding to transducin: a comparative study between meta II intermediates of iodopsin and rhodopsin. Biochemistry 1994;33:4940–4946. [PubMed: 8161555]
17. Burns ME, Mendez A, Chen J, Baylor DA. Dynamics of cyclic GMP synthesis in retinal rods. Neuron 2002;36:81–91. [PubMed: 12367508]
18. Mendez A, et al. Role of guanylate cyclase-activating proteins (GCAPS) in setting the flash sensitivity of rod photoreceptors. Proc. Natl. Acad. Sci. USA 2001;98:9948–9953. [PubMed: 11493703]
19. Lem J, Applebury ML, Falk JD, Flannery JG, Simon MI. Tissue-specific and developmental regulation of rod opsin chimeric genes in transgenic mice. Neuron 1991;6:201–210. [PubMed: 1825171]
20. Luo DG, Yau K-W. Rod sensitivity of neonatal mouse and rat. J. Gen. Physiol 2005;126:263–269. [PubMed: 16129773]
21. Nakatani K, Tamura T, Yau K-W. Light adaptation in retinal rods of the rabbit and two other nonprimate mammals. J. Gen. Physiol 1991;97:413–435. [PubMed: 2037836]
22. Tamura T, Nakatani K, Yau K-W. Calcium feedback and sensitivity regulation in primate rods. J. Gen. Physiol 1991;98:95–130. [PubMed: 1719127]
23. Rieke F, Baylor DA. Origin and functional impact of dark noise in retinal cones. Neuron 2000;26:181–186. [PubMed: 10798402]
24. Shi G, Yau KW, Chen J, Kefalov VJ. Signaling properties of a short-wave cone visual pigment and its role in phototransduction. J. Neurosci 2007;27:10084–10093. [PubMed: 17881515]
25. Sakurai K, et al. Physiological properties of rod photoreceptor cells in green-sensitive cone pigment knock-in mice. J. Gen. Physiol 2007;130:21–40. [PubMed: 17591985]
26. Sampath AP, Baylor DA. Molecular mechanism of spontaneous pigment activation in retinal cones. Biophys. J 2002;83:184–193. [PubMed: 12080111]
27. Bridges CDB. Spectroscopic properties of porphyropsins. Vision Res 1967;7:349–369. [PubMed: 5613301]
28. Donner K, Firsov ML, Govardovskii VI. The frequency of isomerization-like “dark” events in rhodopsin and porphyropsin rods of the bull-frog retina. J. Physiol. (Lond.) 1990;428:673–692. [PubMed: 2231428]
29. Ala-Laurila P, Donner K, Crouch RK, Cornwall MC. Chromophore switch from 11-*cis*-dehydroretinal (A2) to 11-*cis*-retinal (A1) decreases dark noise insalamander red rods. J. Physiol. (Lond.) 2007;585:57–74. [PubMed: 17884920]
30. Kefalov VJ, et al. Breaking the covalent bond – a pigment property that contributes to desensitization in cones. Neuron 2005;46:879–890. [PubMed: 15953417]
31. Dunn FA, Lankheet MJ, Rieke F. Light adaptation in cone vision involves switching between receptor and post-receptor sites. Nature 2007;449:603–607. [PubMed: 17851533]
32. Tachibanaki S, Shimauchi-Matsukawa Y, Arinobu D, Kawamura S. Molecular mechanisms characterizing cone photoresponses. Photochem. Photobiol 2007;83:19–26. [PubMed: 16706600]
33. Nakatani K, Yau KW. Sodium-dependent calcium extrusion and sensitivity regulation in retinal cones of the salamander. J. Physiol. (Lond.) 1989;409:525–548. [PubMed: 2479741]
34. Miller JL, Picones A, Korenbrot JI. Differences in transduction between rod and cone photoreceptors: an exploration of the role of calcium homeostasis. Curr. Opin. Neurobiol 1994;4:488–495. [PubMed: 7812136]
35. Ma J, et al. A visual pigment expressed in both rod and cone photoreceptors. Neuron 2001;32:451–461. [PubMed: 11709156]

36. Perry RJ, McNaughton PA. Response properties of cones from the retina of the tiger salamander. J. Physiol. (Lond.) 1991;433:561–587. [PubMed: 1841958]

37. Wang Y, et al. A locus control region adjacent to the human red and green visual pigment genes. Neuron 1992;9:429–440. [PubMed: 1524826]

38. MacKenzie D, Arendt A, Hargrave P, McDowell JH, Molday RS. Localization of binding sites for carboxyl terminal specific anti-rhodopsin monoclonal antibodies using synthetic peptides. Biochemistry 1984;23:6544–6549. [PubMed: 6529569]

39. Molday LL, Cook NJ, Kaupp UB, Molday RS. The cGMP-gated cation channel of bovine rod photoreceptor cells is associated with a 240-kDa protein exhibiting immunochemical cross-reactivity with spectrin. J. Biol. Chem 1990;265:18690–18695. [PubMed: 1698790]

40. Harosi F. Absorption spectra and linear dichroism of some amphibian photoreceptors. J. Gen. Physiol 1975;66:357–382. [PubMed: 808586]

41. Govardovskii VI, Fyhrquist N, Reuter T, Kuzmin DG, Donner K. In search of the visual pigment template. Vis. Neurosci 2000;17:509–528. [PubMed: 11016572]

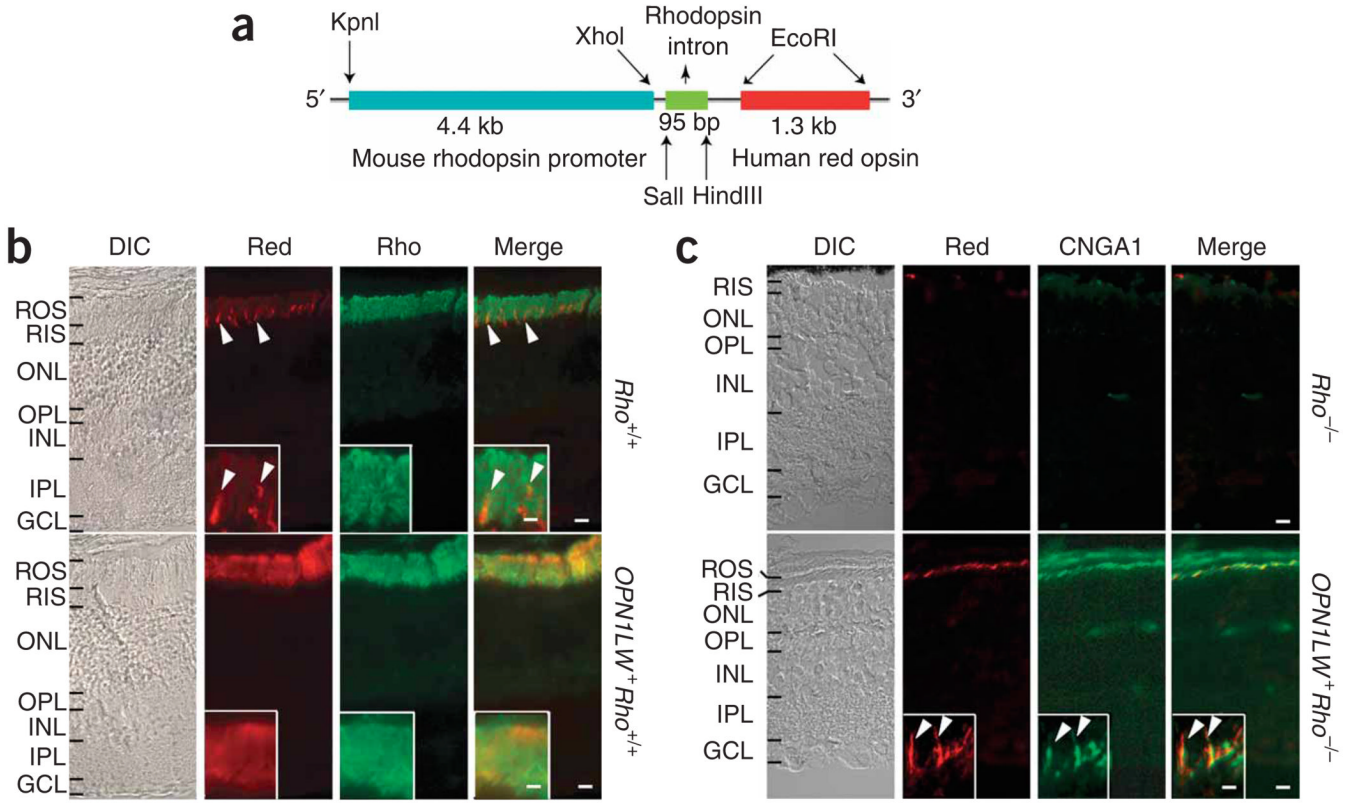

Figure 1.

Mouse rods expressing transgenic human red cone pigment. (**a**) Transgene construct. The 4.4-kb mouse rhodopsin promoter fragment was linked to a 1.3-kb cDNA coding for human red cone opsin. The third intron of the human rhodopsin gene was inserted between the two to improve expression. (**b**) Frozen sections from *Rho*$^{+/+}$ (wild type) and *OPN1LW*$^{+}$ *Rho*$^{+/+}$ (transgenic) mouse retinas immunostained for red cone pigment (red) and rhodopsin (rho). Arrowheads, sporadic mouse cones (presumably green cones) in *Rho*$^{+/+}$ retina cross-labeled by the antibody. Inset, high-magnification view of outer segment layer. DIC, differential interference contrast. (**c**) Frozen sections from 2-month-old *Rho*$^{-/-}$ and *OPN1LW*$^{+}$ *Rho*$^{-/-}$ (transgenic without rhodopsin) mouse retinas immunostained for red cone pigment and rod marker CNGA1. Note the absence of an outer segment layer in *Rho*$^{-/-}$ retina and its presence, although it is thin, in *OPN1LW*$^{+}$ *Rho*$^{-/-}$ retina. Inset, high-magnification view of *OPN1LW*$^{+}$*Rho*$^{-/-}$ rod outer segments with red cone pigment (arrowheads). ROS, rod outer segment; RIS, rod inner segment; ONL, outer nuclear layer; OPL, outer plexiform layer; INL, inner nuclear layer; IPL, inner plexiform layer; GCL, ganglion cell layer. Scale bars: 10 μm in main panels, 2 μm in insets.

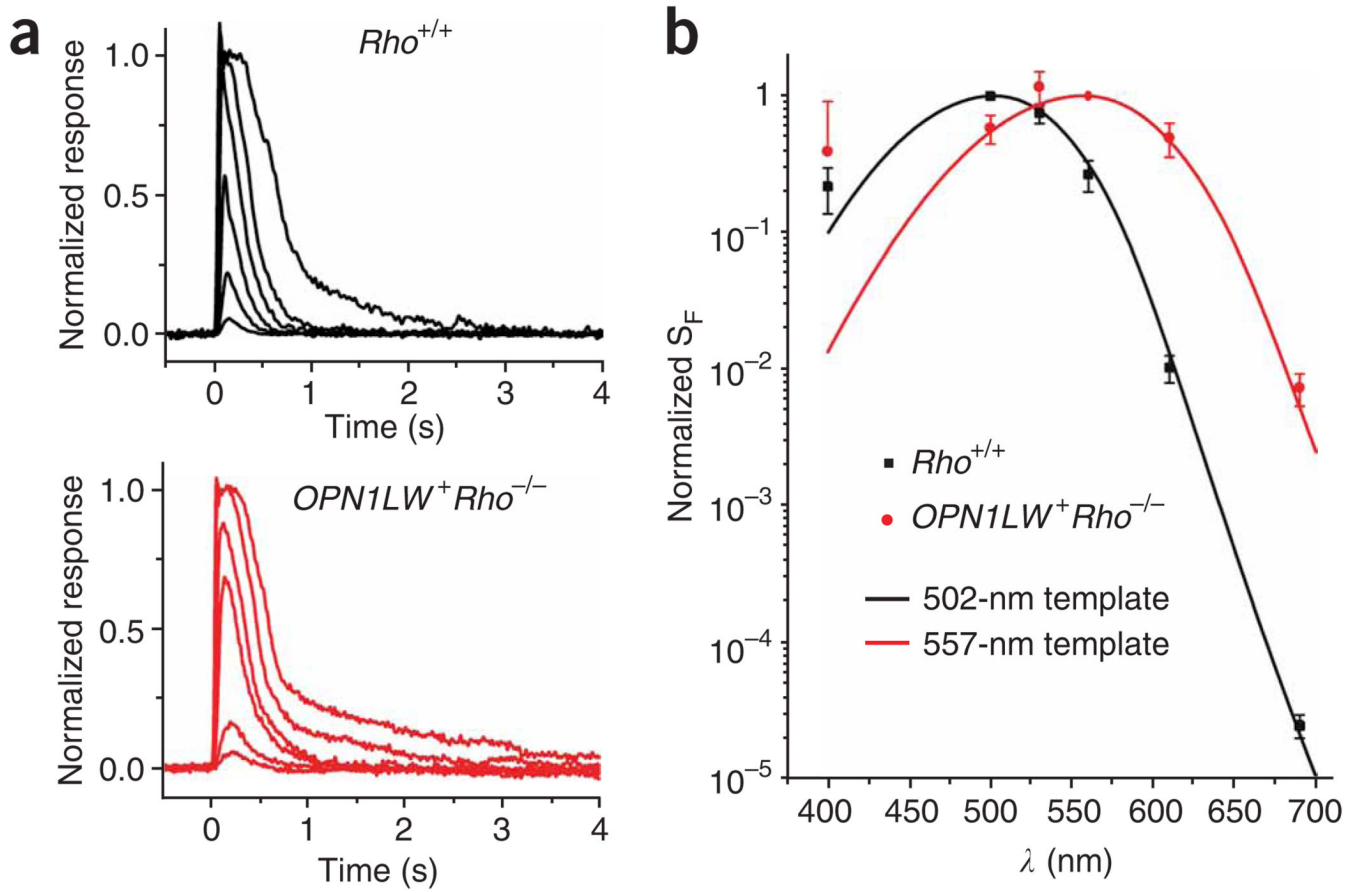

Figure 2.

Responses and action spectrum of mouse rods expressing transgenic red cone pigment. (**a**) Flash intensity-response families from *Rho*$^{+/+}$ and *OPN1LW*$^{+}$ *Rho*$^{-/-}$ rods. A 20-ms flash at $t = 0$ s, delivering 7, 37, 123, 472, 1,589 and 10,281 photons (500 nm) per μm^2 for *Rho*$^{+/+}$ rods (top) and 640, 2,110, 13,339, 43,997, 166,044 and 547,677 photons (560 nm) per μm^2 for *OPN1LW*$^{+}$ *Rho*$^{-/-}$ (bottom). (**b**) Action spectra of *Rho*$^{+/+}$ and *OPN1LW*$^{+}$ *Rho*$^{-/-}$ rods, fit by the absorption-spectrum templates[41] for mouse rhodopsin (λ_{max} = 502 nm) and human red cone pigment (λ_{max} = 557 nm), respectively. Averaged data from 10 *Rho*$^{+/+}$ rods and 24 *OPN1LW*$^{+}$ *Rho*$^{-/-}$ rods. Error bars, s.e.m. Note that the lack of good fit of the data at 400 nm by the templates was due to the presence of the beta-band (with a peak more blue-shifted than λ_{max}) in pigment absorption, traditionally not considered in the spectral templates[41].

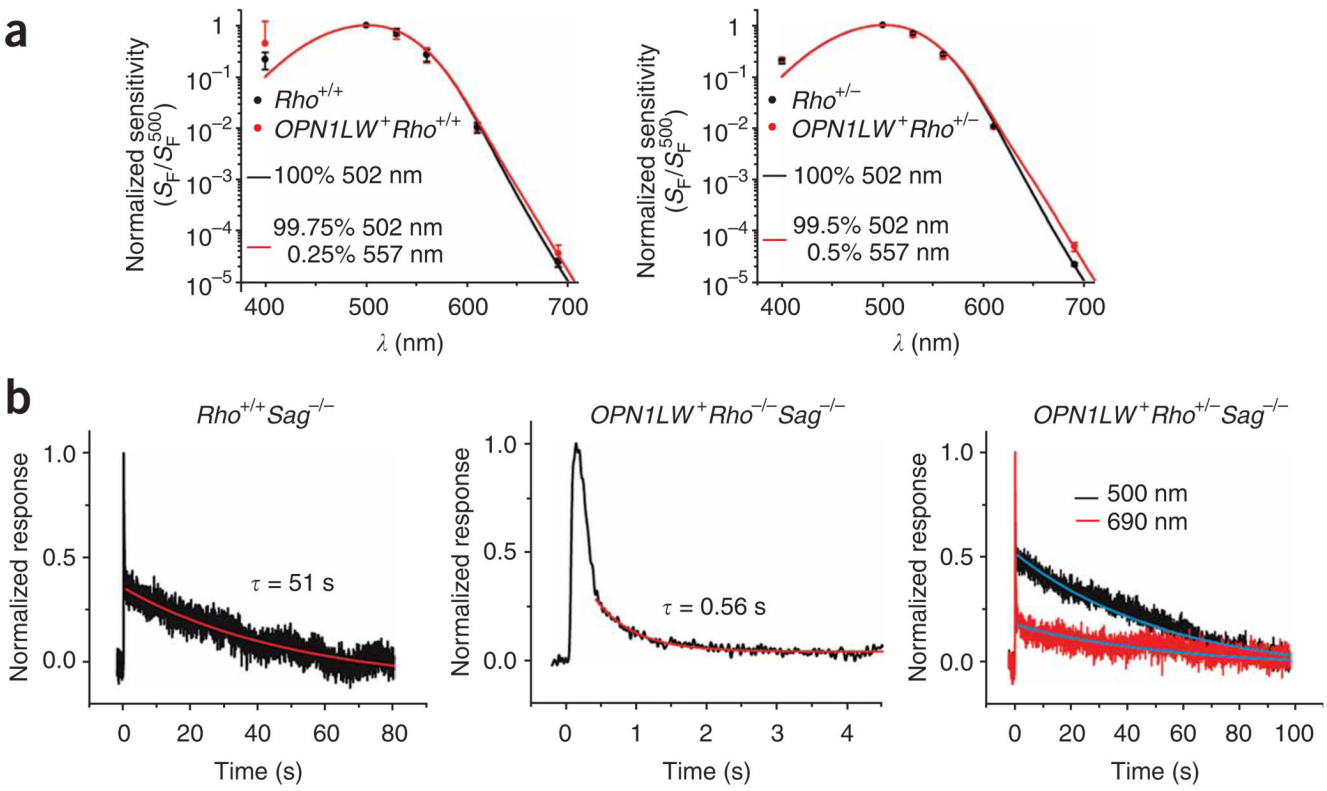

Figure 3.

Estimate of percentage of red cone pigment in transgenic mouse rods. (**a**) Red shift in action spectrum induced by the presence of human red cone pigment in *OPN1LW*$^+$*Rho*$^{+/+}$ rods (n = 11) compared to *Rho*$^{+/+}$ (n = 10) (left), and *OPN1LW*$^+$ *Rho*$^{+/-}$ rods (n = 14) compared to *Rho*$^{+/-}$ (n = 11) (right). Dim-flash sensitivity, S_F, was derived from dim flashes at 400, 500, 530, 560, 610 and 690 nm. Error bars, s.e.m. The action spectra are fit by the indicated linear combinations of the spectral templates for rhodopsin and red cone pigment (see Fig. 2b). (**b**) Averaged flash responses of mouse rods in the absence of arrestin. Left, *Rho*$^{+/+}$ *Sag*$^{-/-}$ rod; 27 flashes, each 25 photons (500 nm) per μm^2. Middle, *OPN1LW*$^+$*Rho*$^{-/-}$*Sag*$^{-/-}$ rod; 30 flashes, each 23,300 photons (560 nm) per μm^2. Red traces, single-exponential declines, with time constant τ = 51 s on left and 0.56 s in middle. Right, *OPN1LW*$^+$ *Rho*$^{+/-}$*Sag*$^{-/-}$ rod. Flashes (15 per wavelength) of 85 photons per μm^2 at 500 nm (black) and 696,123 photons per μm^2 at 690 nm (red).

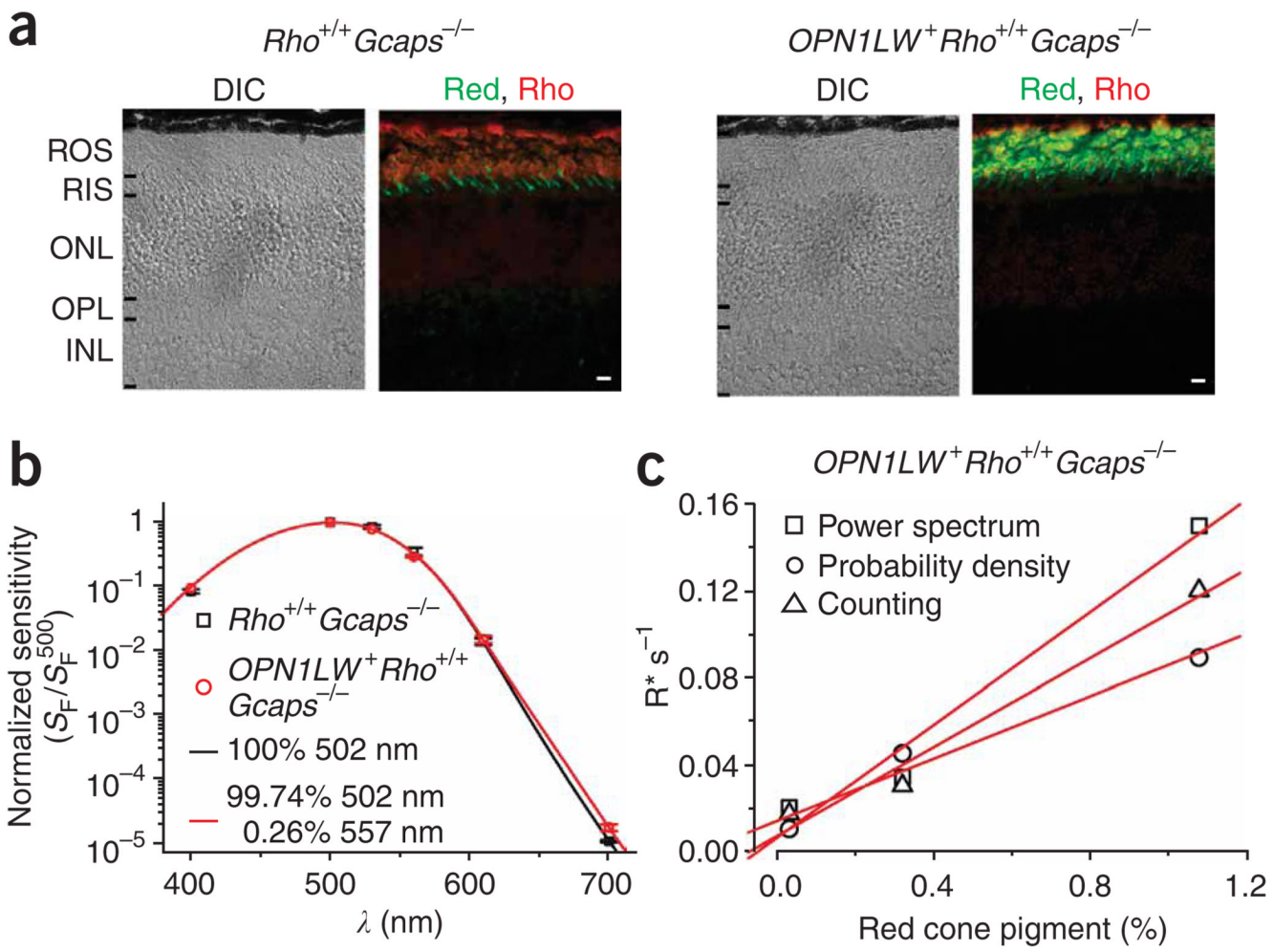

Figure 4.

Expression of human red cone pigment in *Rho*$^{+/+}$ *Gcaps*$^{-/-}$ background. (**a**) Retinal cross-sections from 1-month-old *Rho*$^{+/+}$*Gcaps*$^{-/-}$ and *OPN1LW*$^{+}$ *Rho*$^{+/+}$*Gcaps*$^{-/-}$ mice. Double immunolabeling with antibodies to red cone pigment (green color) and rhodopsin (red color). Scale bar, 10 μm; abbreviations as in Figure 1. (**b**) Estimate of percentage of transgenic red cone pigment in *OPN1LW*$^{+}$*Rho*$^{+/+}$*Gcaps*$^{-/-}$ rods based on the red-shift in the action spectrum. At each wavelength, the responses to 50 dim 10-ms flashes were averaged. Error bars, s.e.m. Altogether, we studied 13 *Rho*$^{+/+}$*Gcaps*$^{-/-}$ and 16 *OPN1LW*$^{+}$ *Rho*$^{+/+}$*Gcaps*$^{-/-}$ rods. Not all indicated wavelengths were examined for every cell, but at least 500 nm and 700 nm were. The wavelengths and the numbers of cells studied (given as λ, number of *Rho*$^{+/+}$*Gcaps*$^{-/-}$ rods, number of *OPN1LW*$^{+}$ *Rho*$^{+/+}$*Gcaps*$^{-/-}$ rods) were, for 500 nm, 13, 16; 700 nm, 13, 16; 610 nm, 8, 6; 560 nm, 7, 2; 530 nm, 9, 1; 400 nm, 3, 1. Note that the apparent good fit of the data at 400 nm by the templates was a coincidence (see Fig. 2b legend; compare to Fig. 2b and Fig 3a) owing to only three cells being studied at this wavelength (see Methods). (**c**) Correlation between cone-pigment expression and the isomerization rate in darkness measured as illustrated in Figure 5 for three *OPN1LW*$^{+}$ *Rho*$^{+/+}$*Gcaps*$^{-/-}$ rods from which both parameters were measured. The dark quantal rate included events originating from the endogenous rhodopsin.

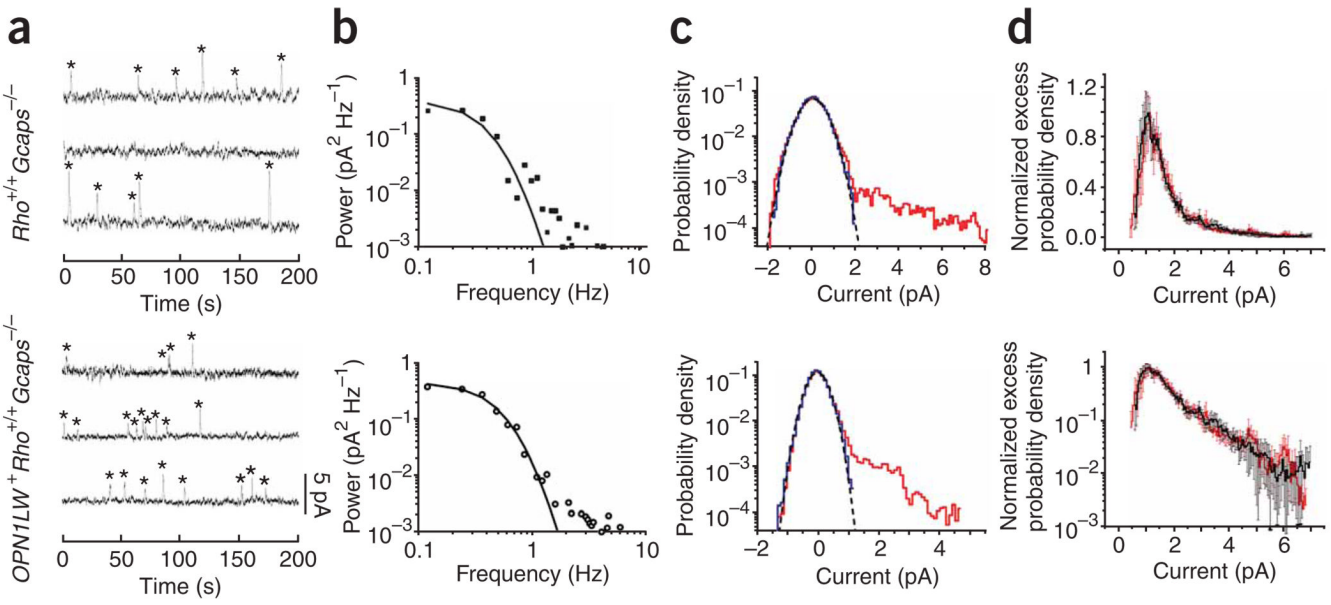

Figure 5.

Measurement of spontaneous isomerization rate of red cone pigment. (**a–c**) Top, same *Rho*$^{+/+}$ *Gcaps*$^{-/-}$ rod (control). Bottom, same OPN1LW^{+} *Rho*$^{+/+}$*Gcaps*$^{-/-}$ rod. See text and Methods for details. (**a**) Counting method. Sample recordings (continuous in time from top through bottom traces) in darkness showing discrete events (asterisks) identified based on a criterion amplitude of >30% of single-photon response. (**b**) Method based on power-density spectra. Difference power spectrum (spectrum with events minus spectrum without events) fitted by that for the single-photon response function. (**c**) Probability density method. Red profile, probability density histogram of overall dark recordings. Bin width, 0.1 pA. Blue profile is that of selected recording segments with no apparent events, scaled to the same height as the red profile. Black dashed curve, scaled gaussian distribution that fits the negative sides of the red and blue histograms. (**d**) Overlaid (and normalized to the same height) excess probability density histograms averaged from six *Rho*$^{+/+}$*Gcaps*$^{-/-}$ (red) and six *OPN1LW*$^{+}$ *Rho*$^{+/+}$*Gcaps*$^{-/-}$ (black) rods to show their identical profiles. Top, linear coordinates; bottom, semilog. Bin width, 0.05 pA; error bars, s.e.m.

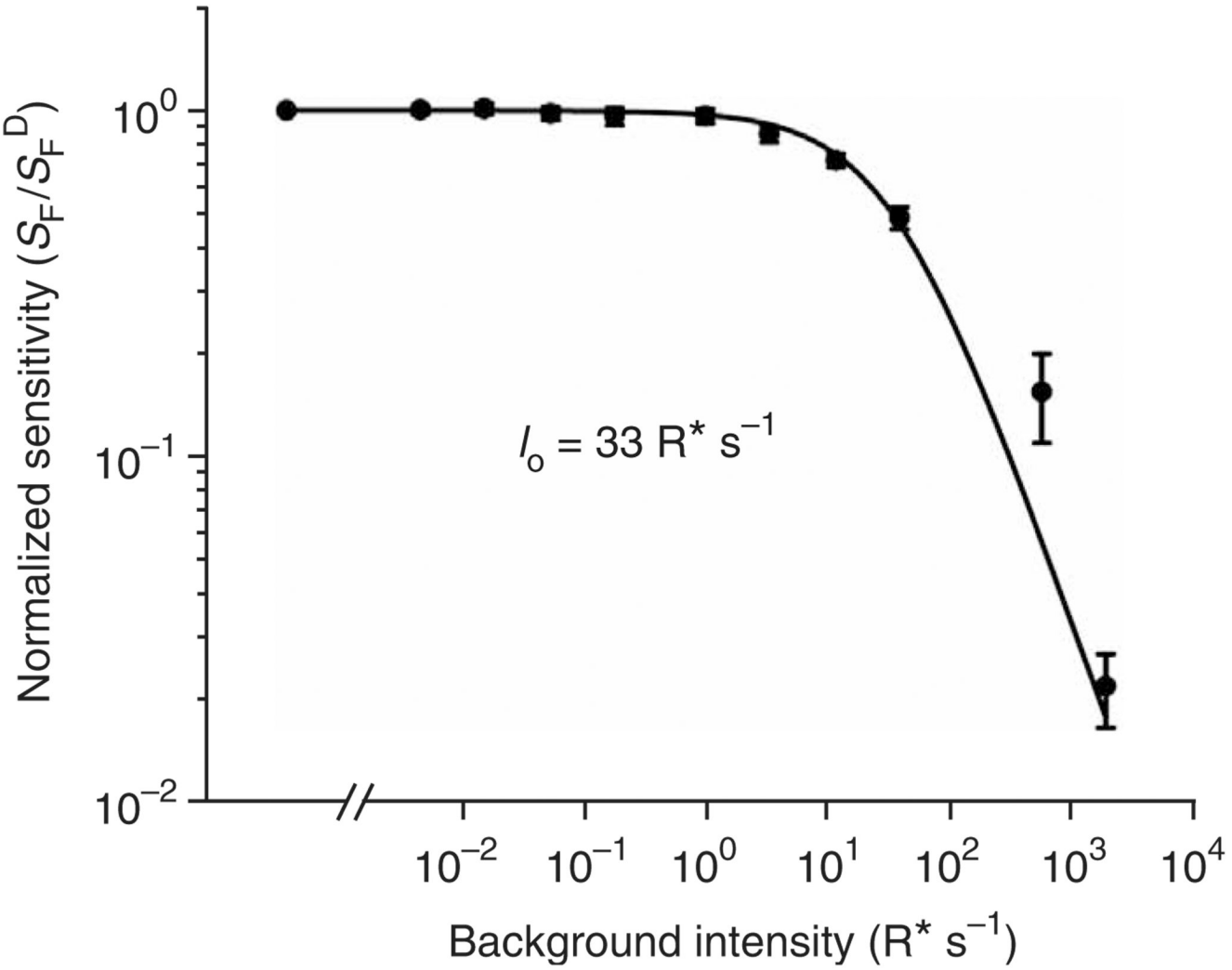

Figure 6.

Background adaptation of wild-type (*Rho*$^{+/+}$) mouse rods. Plot of normalized flash sensitivity against number of isomerizations per second due to background light intensity. Averaged results from 11 cells. Continuous curve is from Weber-Fechner relation, $S_F = S_F^D I_o/(I_B + I_o)$. S_F^D, flash sensitivity in the absence of background light; S_F, flash sensitivity in the presence of a background light I_B; I_o, the background intensity required to reduce the rod sensitivity to half of its dark value. Error bars, s.e.m. See text for details.

Table 1

Parameters of flash responses of control mouse rods and transgenic mouse rods expressing human red cone pigment

	Rho$^{+/+}$	**Rho$^{+/-}$**	**OPN1LW^{+}Rho$^{-/-}$**	**OPN1LW^{+}Rho$^{+/+}$**	**OPN1LW^{+}Rho$^{+/-}$**
S_F (pA photon^{-1} μm^2)	(18.0 ± 3.0) × 10^{-2}	(9.0 ± 1.0) × 10^{-2}	(9.3 ±0.2) × 10^{-4}	(15.0 ± 4.0) × 10^{-2}	(12.0 ± 5.0) × 10^{-2}
	500 nm (n = 11)	500 nm (n = 10)	560 nm (n = 24)	500 nm (n = 11)	500 nm (n = 14)
a (pA)	0.40 ± 0.03 (n =10)	0.27 ± 0.05 (n =11)	0.35 ± 0.03 (n =25)	0.38 ± 0.03 (n =10)	0.28 ± 0.06 (n =11)
t_p (ms)	177 ± 5 (n =10)	147 ± 8 (n =11)	239 ± 18 (n =25)	155 ± 9 (n =10)	149 ± 8 (n =11)
t_i (ms)	267 ± 33 (n =7)	253 ± 29 (n =11)	499 ± 37 (n =25)	228 ± 16 (n =10)	255 ± 20 (n =11)

Values are mean ± s.e.m., with the number of cells studied indicated in parentheses. S_F is flash sensitivity at indicated wavelength (corresponding to λ_{max}); a is the amplitude of the single-photon response; t_p and t_i are time to peak and integration time of the dim-flash response, respectively (all probed at the indicated wavelengths). The low (~0.5%) S_F of *OPN1LW^{+} Rho$^{-/-}$* rods compared to *Rho$^{+/+}$* rods was due to the low expression of red cone pigment in the outer segment (see main text). The response kinetics was also slower than in wild type, probably because of the outer-segment morphology of surviving rods in the degenerating retina not being entirely normal.

Nat Neurosci. Author manuscript; available in PMC 2009 November 9.